uro

MDPI

Brief Report

The Porcine Model for Urological Research and Training: An Endoscopic and CT-Based Study

Jeff John [1,2,*], Graham Fieggen [3], Lisa Kaestner [1] and John Lazarus [1]

[1] Division of Urology, Department of Surgery, Groote Schuur Hospital and University of Cape Town, Cape Town 7925, South Africa
[2] Division of Urology, Department of Surgery, Frere Hospital and Walter Sisulu University, East London 5201, South Africa
[3] Division of Neurosurgery, Department of Surgery, Groote Schuur Hospital and University of Cape Town, Cape Town 7925, South Africa
* Correspondence: jeffveenajohn@gmail.com; Tel.: +27-437092111

Abstract

Background/Objectives: For centuries, humans have employed animal models to progress biomedical science, to understand pathological and biological processes, and to develop and test drugs, vaccines, and surgical techniques. In the field of urology, Sampaio and his colleagues from Brazil were the pioneers in proposing that the porcine model is the most accurate representation of the human kidney. We aim to describe the relevant urinary anatomy of female Landrace pigs based on endoscopy and computed tomography (CT) scans and compare differences between the urinary anatomy of pigs and humans. **Methods**: Four white Landrace female pigs were used for the study: two for CT imaging and two for endoscopic assessment. CT-urograms were performed using a 64-channel tomography machine with 0.625 mm thick slices. For the endoscopic procedure, the intravaginal urethral meatus was cannulated using a cystoscope, followed by complete urethrocystoscopy. The ureteric orifices were then cannulated, and a retrograde pyelogram was performed, followed by ureterorenoscopy. The analyses were performed using SPSS (Version 28), and simulated data was created using R (version 3.5.0), with the significance set at $p \leq 0.05$. The data obtained from two pigs was used to simulate an empirical data with 500 observations, using the mean and standard deviations from our $n = 2$ to produce a random normal distribution. **Results**: CT and endoscopic findings showed two multirenculate multipapillate kidneys, each receiving blood supply from a single renal artery that is further divided into cranial and caudal branches. The delayed phase of the urogram showed distal ureters passing posterior to the bladder and emptying into the bladder at the base. Urethroscopy revealed an intravaginal urethral meatus ventral to the anus, positioned midway between the mucocutaneous junction of the vulva and the cervix. Endoscopic view of the bladder neck showing patulous ureteric orifices at the bladder neck with no distinct interureteric ridge or trigone. Retrograde pyelogram showed a Group B drainage pattern in both pigs. **Conclusions**: While there are numerous similarities between the urinary systems of humans and pigs, there are important subtle differences that urologists and researchers need to be mindful of before using the porcine model for urological research and training.

Keywords: endourology; flexible ureteroscopy; porcine model; pig model; retrograde intrarenal surgery

Check for updates

Academic Editor: Tommaso Cai

Received: 17 January 2026
Revised: 18 February 2026
Accepted: 27 February 2026
Published: 3 March 2026

Copyright: © 2026 by the authors. Licensee MDPI, Basel, Switzerland. This article is an open access article distributed under the terms and conditions of the Creative Commons Attribution (CC BY) license.

1. Introduction

For centuries, humans have employed animal models to progress biomedical science, to understand pathological and biological processes, and to develop and test drugs, vaccines, and surgical techniques [1]. Research on cows helped create the world's first vaccine to eradicate smallpox [2]; in the 1940s and the 1950s, several monkeys died to develop the polio vaccine [3]. Professor Christian Barnard, who pioneered the first human heart transplant, initially gained expertise in orthotopic heart transplantation in canines [3]. The use of pigs in scientific studies, particularly as preclinical models, has experienced a significant surge since the early 1980s. Pigs exhibit a high degree of biological similarity to humans when considering their anatomical and physiological characteristics [4]. Furthermore, there is a wealth of information available about their unique behavioural and husbandry considerations and reproductive management [5]. They are also an economically viable and freely available model due to the widespread commercial breeding for the meat industry [6]. In the field of urology, Sampaio and his colleagues from Brazil were the pioneers in proposing that the porcine model is the most accurate representation of the human kidney [7]. Since then, the porcine model has been extensively utilised for endourological training, device evaluation, and translational research. Nonetheless, despite its widespread use, important uncertainties remain regarding the detailed anatomy of the porcine urinary tract. The majority of the existing literature emphasises renal architecture, while there is a relative paucity of high-resolution anatomical correlations concerning the ureters, bladder, and urethra. Moreover, inconsistencies have been documented concerning ureteral length, ureteric orifice morphology, bladder capacity, and urethral dimensions. A further drawback in the current literature is that anatomical descriptions frequently originate from cadaveric dissection, solitary imaging investigations, or endoscopic views conducted independently. Limited studies have integrated cross-sectional imaging with direct endoscopic evaluation to provide a comprehensive, clinically relevant anatomical correlation. This paper describes the relevant urinary anatomy of female Landrace pigs based on endoscopy and computed tomography (CT) scans. It also examines the parallels and differences between the urinary anatomy of pigs and humans. This multimodal assessment is crucial for precisely characterising spatial connections, luminal morphology, and anatomical variability—elements that directly influence the feasibility and reproducibility of experimental and training protocols.

2. Materials and Methods

Ethical Approval: The local Animal Ethics Committee (AEC) approved the study (AEC 020_011). Veterinary and paraveterinary specialists were employed to guarantee the well-being and clinical care of the animals. Four white Landrace female pigs (weight 50–60 kg) were used in this study. Two were utilised for CT imaging, while an additional two were employed for endoscopic evaluation. The animals were brought to the research facility and boarded for seven days to allow a sufficient acclimatization period. The pigs were provided with a regular diet for up to 12 h before the study, but access to water was not restricted at any point.

Study Design: This is a prospective descriptive experimental anatomical study using a porcine model with multimodal imaging and endoscopic assessment.

Anaesthetic protocol: Identical anaesthetic methods were used for both the CT scans and endoscopic procedures. Prior to the procedure, the pigs were administered a diazepam patch for pre-medication. They were then induced with a mixture of Zoletil (3 mg/kg IM), Medetomidine (0.06 mg/kg IM), and Butorphanol (0.15 mg/kg IM) and then intubated and ventilated, with anaesthesia being maintained using isoflurane (1.5–3% in oxygen) The animals were initially hydrated with a saline bolus of 90 mL/kg, given over 5 min.

Hydration was maintained during the surgery by administering saline (10 mL/kg/h) through an ear vein.

Computed tomography (CT) assessment: CT urograms were performed using a 64-channel tomography machine with 0.625 mm thick slices. The dual-phase study included an initial 50 mL bolus of intravenous non-ionic iodinated contrast. After ten minutes, an arterial (corticomedullary) and nephrographic (parenchymal) assessment was performed using 100 mL of contrast medium to optimally evaluate the arterial and venous structures. This was followed by an excretory (delayed) study performed after ten minutes for optimal evaluation of the ureters and bladder. The following parameters were measured:

(a) Renal length: the distance measured along the long-axis of the kidney, i.e., the greatest distance between the cranial and caudal edges.
(b) Cranial and caudal pole width: from an axis, perpendicular to the length, drawn at the broadest segment of the cranial and caudal renal poles.
(c) Kidney and bladder volumes: measured using the region of interest (ROI) tool.
(d) Ureteral length: the sum of the length of the abdominal ureter (ureteropelvic junction to pelvic brim) and pelvic ureter (pelvic brim to ureterovesical junction).

Endoscopic assessment: The pigs were positioned in the dorsal lithotomy position. A single-use cystoscope (9F, WiScope®, OTU Medical (Union City, CA, USA)) was introduced into the vagina to locate the urethral meatus. The cystoscope was then advanced into the bladder, and following a thorough examination, the ureteral openings were located and cannulated using conventional guidewires (0.035 inch) with the assistance of fluoroscopy. The guidewire was exchanged for an open-ended ureteric catheter (6F) through which contrast was administered to completely opacify the ureter and renal collecting system (retrograde pyelogram) to determine the calyceal configuration according to the Sampaio classification. The open-ended ureteric catheter was exchanged for a standard guidewire, over which a single-use ureteroscope (7.4 Fr, WiScope®, OTU Medical) was advanced to facilitate a complete renoscopy and ureteroscopy. The procedure was then repeated on the opposite side. After completing the assessment and determining that the pig model was suitable for urological research, the researchers proceeded to use the same animals to pilot a novel drug eluting guidewire to enhance the endoscopic management of renal stones [8,9].

Statistical analysis: The analyses were performed using SPSS (Version 28), and simulated data was created using R (version 3.5.0), with the significance set to $p \leq 0.05$. The data obtained data from 2 pigs was used to simulate empirical data with 500 observations, using the mean and standard deviations from our n = 2 sample to produce a random normal distribution. The normality of these distributions was verified using the Shapiro–Wilk test. The mean, standard deviation and coefficient of variation were determined for all datasets. Dependent sample *t*-tests compared the left and right data distributions. As this was a descriptive feasibility anatomical study, a formal power calculation was not performed. The sample size was determined based on ethical considerations and adherence to the principles of animal research minimisation. We agree that for hypothesis-driven comparative studies, formal power analysis is essential, and this will be incorporated in future confirmatory investigations.

3. Results

Computed tomography (CT) and endoscopy (including retrograde pyelography) showed two multirenculate, multipapillate kidneys, each receiving blood supply from a single renal artery that divides into cranial and caudal branches. In the right kidney of pig 1, there was an incidental finding of a large (2 × 2.5 cm) parapelvic cyst (Figure 1).

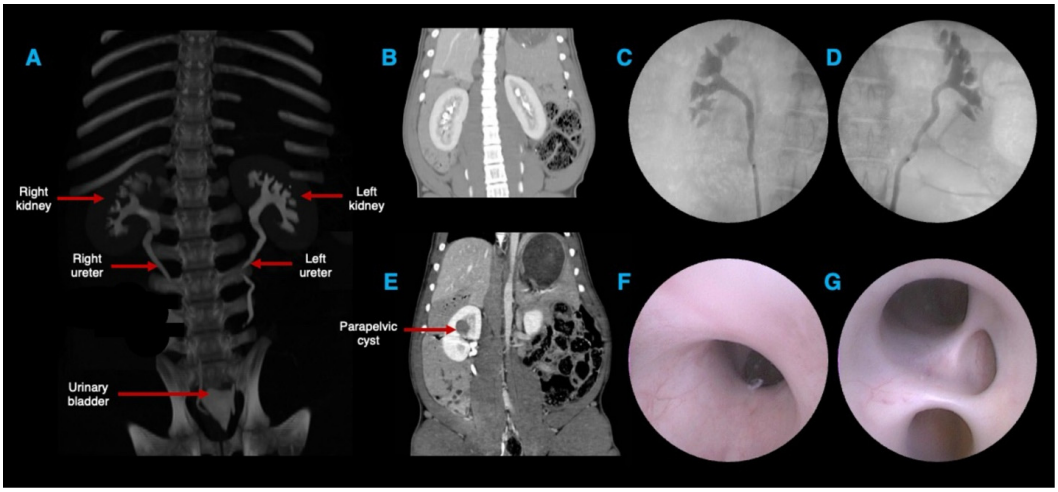


Figure 1. CT urogram and retrograde pyelogram images of the upper urinary tract showing two multirenculate, multipapillate kidneys and their corresponding ureters (**A**–**E**). Endoscopic view of the renal pelvis from the ureteropelvic junction (**F**) and renal calyces (**G**).

CT measurements for the kidneys, ureters, and bladders of both pigs are summarised in Table 1.

Table 1. CT measurements for the kidneys, ureters, and bladders of both pigs in the study.

Kidneys	Mean	SD	CV %	*t*	*p* Value
Right renal length (cm)	10.82	10.88	100.55	−1.10	0.272
Left renal length (cm)	11.57	11.74	101.47		
Right renal cranial pole width (cm)	5.14	5.00	97.28	2.07	0.019 *
Left renal cranial pole width (cm)	4.52	4.58	101.33		
Right renal caudal pole width (cm)	4.21	4.14	98.34	−2.11	0.018 *
Left renal caudal pole width (cm)	4.77	4.73	99.16		
Right kidney volume (cc)	158.80	160.71	100.55	1.11	0.134
Left kidney volume (cc)	147.80	146.20	101.47		
URETERS	Mean	SD	CV %	*t*	*p* value
Right total ureteral length (cm)	23.15	25.28	109.20	−3.72	<0.001 *
Left total ureteral length (cm)	29.73	29.79	100.20		
Right abdominal ureteral length (cm)	14.94	16.07	107.56	−2.91	0.002 *
Left abdominal ureteral length (cm)	18.11	17.97	99.23		
Right pelvic ureteral length (cm)	9.06	9.53	105.19	−3.01	0.001 *
Left pelvic ureteral length (cm)	10.98	11.45	104.28		
Kidneys	Mean	Median	SD	CV %	
Bladder volume (cc)	532.50	236.88	532.50	44.48	

SD—standard deviation; CV—coefficient of variation; cm—centimetre; cc—cubic centimetre; *—statistically significant.

The renal length was, on average, 10.82 cm on the right and 11.57 cm on the left, with no statistical difference between the sides ($p = 0.272$). The width of the cranial renal pole was, on average, 5.14 cm on the right and 4.52 cm on the left, with the width being significantly higher on the right side ($p = 0.019$). The width of the caudal renal pole was 4.21 cm on the right side and 4.77 cm on the left, with the width being significantly higher

on the left side ($p = 0.018$). The renal volume was 158.8 cm^3 on the right and 147.8 cm^3 on the left, with no statistical difference between the sides ($p = 0.134$).

Both pigs exhibited a Group B pattern of drainage of the pelvi-calyceal system as revealed by the retrograde pyelogram. The total ureteral length varied from 23.15 cm on the right to 29.73 cm on the left, with an average of 30 cm. The total ureteral length was statistically higher on the left side ($p < 0.001$). The abdominal ureteral length was 14.94 cm on the right and 18.11 cm on the left. Abdominal ureteral length was significantly higher on the left side ($p = 0.002$). The pelvic ureteral length was 9.06 cm on the right and 10.98 cm on the left. Pelvic ureteral length was significantly higher on the left side ($p = 0.001$).

In the delayed CT phase, the distal ureters passed posteriorly to the bladder and were emptied into the base of the bladder. Urethroscopy and cystoscopy revealed two patulous ureteric orifices at the bladder neck, 1–3 cm apart in both pigs (Figure 2). No bladder trigones were observed. The estimated bladder volumes were 700 and 365 mL in pig 1 and 2, respectively (Figure 2). The urethral orifice was identified intravaginally (Figure 3).

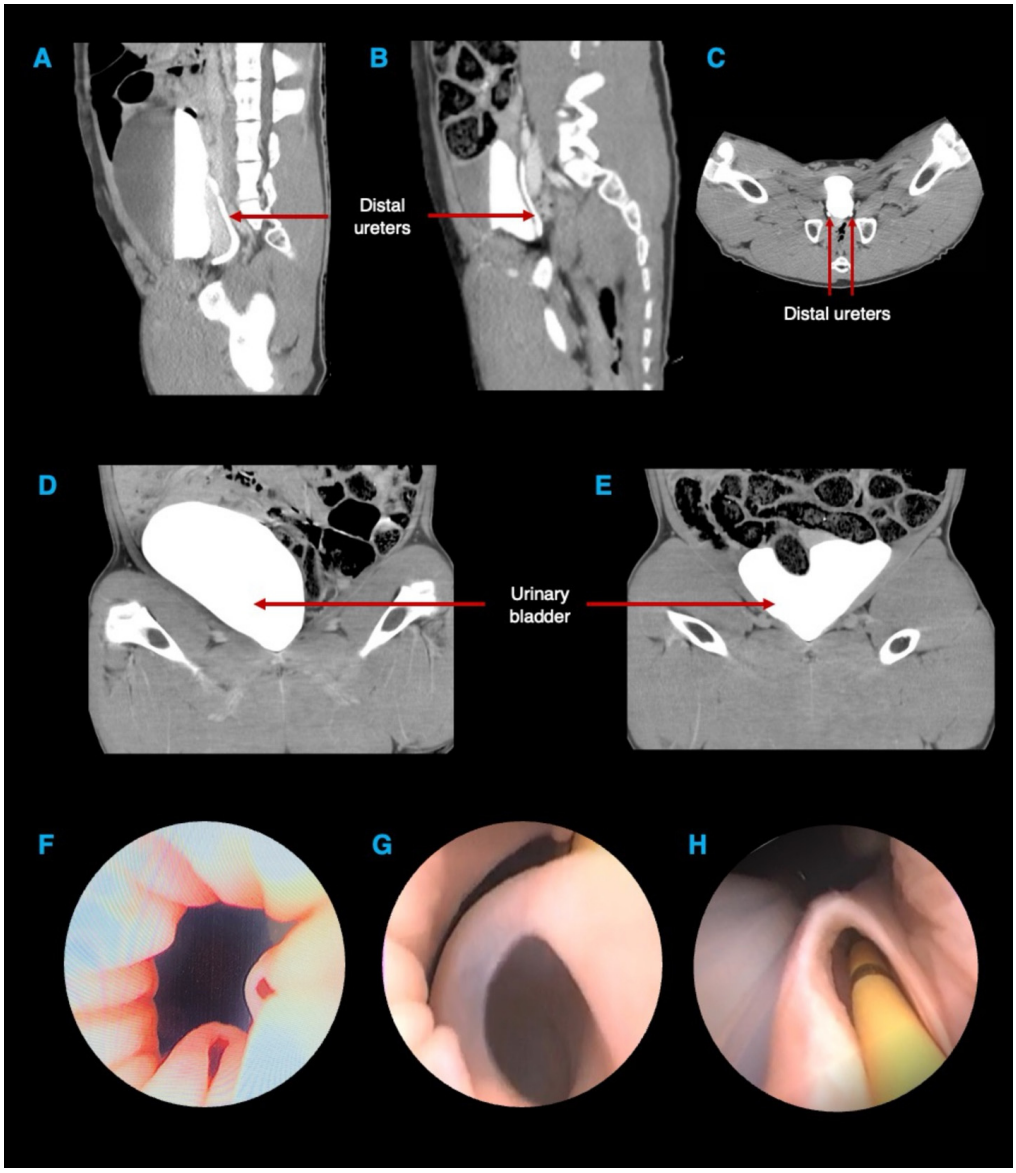


Figure 2. Delayed phase of the CT urogram showing distal ureters (**A**–**C**) passing posteriorly to the bladder and emptying into the bladder (**D**,**E**) at its base. Endoscopic view of the bladder neck showing patulous ureteric orifices at the bladder neck (and no interureteric ridge) (**F**,**G**), which allowed easy passage of a 6F ureteric catheter (**H**).

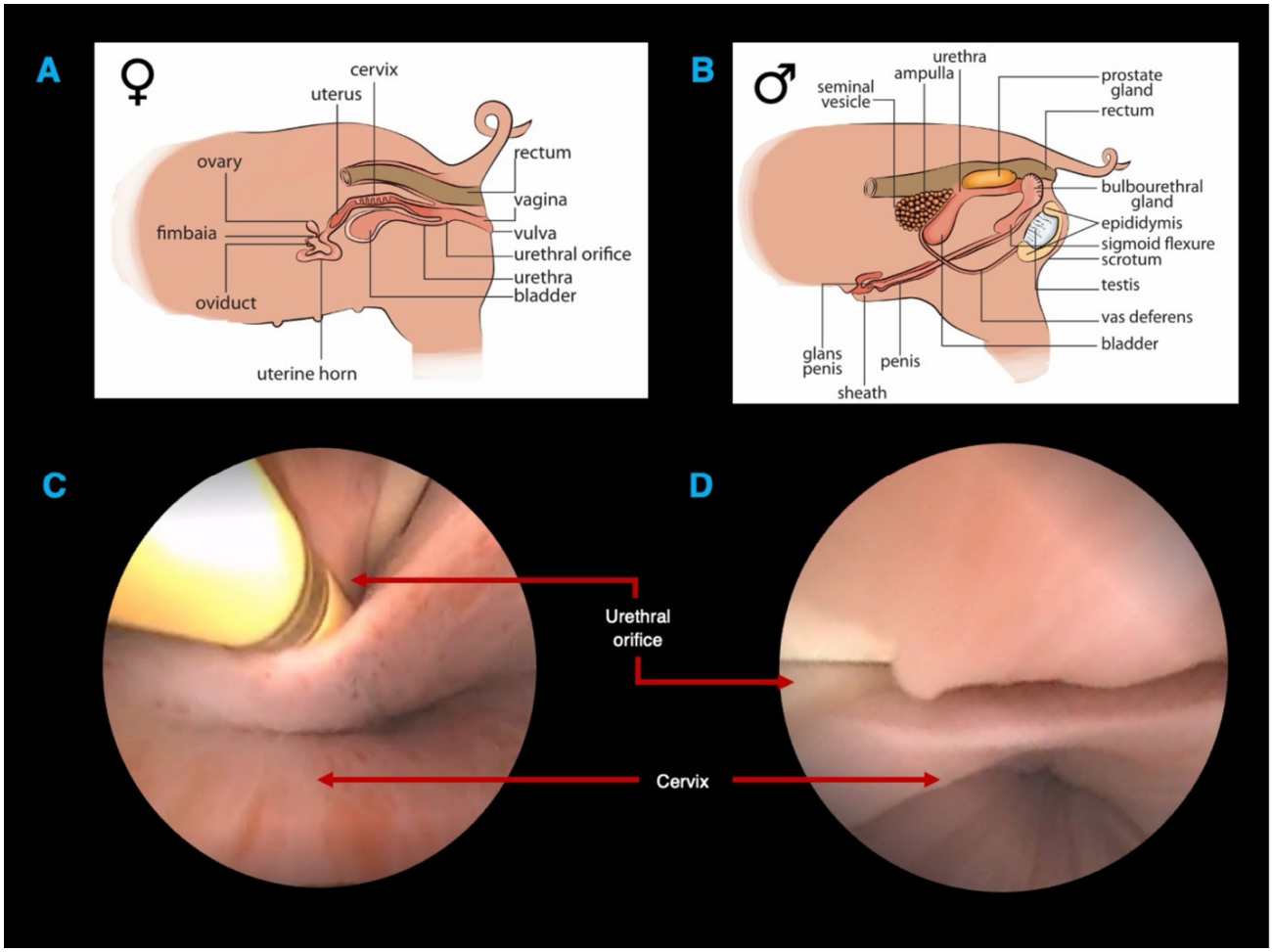


Figure 3. Graphical representation showing the genitourinary anatomy in the female (**A**) and male (**B**) porcine model, noting the position of the urethral orifice. Vaginoscopy showing the urethral opening both with (**C**) and without (**D**) a 6F ureteric catheter and cervical opening.

4. Discussion

The porcine model has often been used by researchers and urological surgeons for advances in medicine. The model has proven ideal for understanding physiological and pathological processes [10], preclinical trials [11] and robotic, laparoscopic, and endourological training [12]. Although the porcine model presents numerous benefits, precise anatomical knowledge that establishes it as the ideal model in urology remains limited. This study is the first to describe the relevant endoscopic and CT-based urological anatomy of female Landrace pigs.

In our study, the mean renal length measured from pole to pole was 10.70 cm on the right side and 11.40 cm on the left side. The measurements fall within the range of what we would expect in a human kidney [13,14]. The plausible hypotheses to account for the discrepancy in size between the two sides is similar to the explanation in humans: the presence of the liver on the right prevents the spatial expansion of the right kidney, and there is increased blood flow to the left kidney due to a shorter left renal artery [15]. Gómez et al. and Arenas et al. reported mean renal lengths of 12 cm in pigs [16,17]. However, the lengths were determined by surgically dissecting the kidneys of various breeds that weighed much more than the pigs used in this study. In humans, the absolute renal length is considered smaller in women [18]. The mean renal lengths in our two female pigs were longer than those measured on CT by other authors in male pigs [19].

Talhar et al. examined the CT scans of 140 anatomically normal kidneys of 70 individuals and reported the mean renal volume to be 94.18 cm^3 and 98.06 cm^3 on the right and left, respectively [20]. The mean renal volumes in our study (157 cm^3 for the right and 147 cm^3 for the left kidney) were much larger. Furthermore, the mean renal volumes in our female pigs were also greater than those measured on CT in male pigs (113.70 cm^3 on the right; 109.70 cm^3 on the left) [19]. Surprisingly, despite the mean renal length of the left kidney being longer in our study, the mean renal volume of the right was higher. These differences are likely due to variations in the size of animals and inter-observer variability while measuring parameters. The presence of a large parapelvic cyst (2×2.5 cm) in the right kidney of one of our pigs could possibly also have likely influenced the measurements.

Researchers who analysed 3-dimensional endocasts of the kidneys noted that each of the pigs had a single artery per kidney. In 93.4% of cases, this artery was divided into cranial and caudal branches, while in 6.6% of cases, it was divided into dorsal and ventral branches [21]. In contrast, humans exhibit multiple renal arteries in almost a third of cases (27–30%) [22]. Prior to entering the renal hilum, the human renal artery undergoes a longitudinal division, resulting in an anterior and posterior division. Each division then divides into segmental arteries. On the other hand, Evan et al. demonstrated that the primary renal artery in pigs divides into two consistent patterns. In the predominant pattern (I), the renal artery in pigs bifurcates into two polar arteries, namely upper and lower, which further divide into anterior and posterior segmental arteries. This anatomically separates the blood flow to the kidney into two separate areas that align with the top and lower sections of the kidney, namely in a transverse direction. In our investigation, we discovered a pattern where additional arteries originating from the lower polar artery also supplied the upper pole [23]. Clinically, the difference in this pattern between human and pig kidneys is important, as the avascular plane in porcine kidneys is transverse, whereas in human kidneys, it is longitudinal.

The kidneys of our pigs exhibited a genuine multirenculate, multipapillate structure, like the calyceal structure found in humans. In their landmark work, Sampaio et al. [24] studied a porcine collecting system by injecting polyester resin into the ureter to completely fill the collecting system. The casts of the collecting system were utilised to classify the pig pelvicalyceal system into two distinct groupings. Group A exhibited two prominent calyceal groups within the pelvicalyceal system, with the draining of the mid-zone relying on either cranial or caudal calyceal drainage. In Group B, the mid-zone drainage was independent of the cranial or caudal calyceal drainage. Sampaio et al. discovered that 40% of pig kidneys displayed Group A drainage and 60% displayed Group B drainage, while 62% of human kidneys exhibited Group A drainage and 38% exhibited Group B drainage, according to this classification. In our study, it was difficult to assess this in the delayed CT phase. However, retrograde pyelogram images suggested a Group B drainage pattern in both pigs. Furthermore, we noted a perpendicular minor calyx that directly drains into the renal pelvis. This particular pattern is found in 18% of pig kidneys, but it is only present in 11.4% of human kidneys [24]. The identification of a Group B drainage pattern has implications for retrograde intrarenal surgery (RIRS), as differences in calyceal orientation and infundibular anatomy may influence scope deflection, stone accessibility, and laser fibre manoeuvrability, thereby affecting procedural realism.

The ureteric orifices drained into the bladder at the bladder neck with roughly 1–3 cm between them. While some authors have described the ureteric orifices as tight [25], we found them to be patulous, enabling smooth insertion of the 7.4 F ureteroscope into the renal pelvis. Endoscopically, we found that there was no bladder trigone, and this agrees with reports from other researchers [26]. The absence of the ureteric orifices at the

trigone and, consequently, the interureteric ridge and Bell's muscle would explain this. The presence of these patulous ureteric orifices and the absence of a well-defined trigone may reduce resistance during ureteric cannulation, potentially facilitating access compared to the human bladder and thereby limiting the fidelity of simulation for early endoscopic skill acquisition. Furthermore, certain anatomical differences may limit the applicability of the porcine model for procedures reliant on trigonal anatomy or ureterovesical junction competence, such as vesicoureteral reflux studies, ureteric reimplantation, or complex reconstructive surgery. Conversely, this configuration may be advantageous for standardised training in guidewire manipulation and ureterorenoscopy without the confounding variable of difficult orifice identification. The anatomical capacity of the bladder gradually rises with age, to a mean between 400 and 600 mL in adulthood [27]. Although our two female pigs had a comparable mean volume of 533 mL, there was a wide range, that is, 700 and 365 mL in pigs 1 and 2, respectively, probably because of the varying degrees of bladder fullness one would expect. The porcine bladder is an intraperitoneal organ, with the entire surface being covered with peritoneum, as opposed to the extraperitoneal/subperitoneal position in humans [28]. Furthermore, the bladder wall is thinner, and care should be taken during urological procedures [29]. Endoscopically and radiologically, it was difficult to confirm these findings.

The human female urethra perforates the urogenital diaphragm, and its external orifice is located right in front of the vaginal opening, making urethral catheterization straightforward. Our examination revealed that the urethral orifice in the female pig was located intravaginally, ventral to the anus, and distally positioned midway between the mucocutaneous junction of the vulva and the cervix (Figure 3). Vaginoscopy was therefore needed to identify the urethral opening and gain access to the urinary tract. In contrast, the male pig has a long, fibroelastic penis with an 'S'-shaped sigmoid flexure ventral to the pubic bone. The tip of the penis is spiral-shaped like a corkscrew, and there is a pouch-like structure called the preputial diverticulum on the underside of the abdomen. These anatomical features make the retrograde passage of catheters or endoscopic tools technically very challenging [29].

Despite subtle difference between the human and porcine anatomy, several similarities make the pig particularly valuable for transluminal and endoscopic procedures, including ureteroscopy, retrograde intrarenal surgery, percutaneous renal access, and the development of novel endourological technologies. In addition, the porcine urinary tract provides a realistic platform for surgical simulation and skills acquisition, allowing trainees to practice instrumentation, navigation of the pelvicalyceal system, and management of intraoperative challenges in a setting that closely approximates human anatomy. A detailed understanding of both the similarities and the subtle anatomical differences is therefore essential to optimise the validity, safety, and translational applicability of this model in experimental research and surgical education.

This study has several limitations that warrant consideration. Most notably, the data was obtained using a small sample size—comprising four animals of one pig breed, divided between two investigative modalities—which limits the ability to assess intraspecies anatomical variability. The limited cohort precludes meaningful evaluation of inter-individual differences in renal morphology, ureteric configuration, and endoluminal dimensions, and therefore restricts generalisability of the findings. However, this investigation was designed as an exploratory anatomical characterisation integrating cross-sectional imaging and endoscopic assessment, rather than as a morphometric prevalence study. Ethical considerations aligned with the principles of reduction in animal research, together with logistical and resource constraints, necessitated the use of a minimal number of animals. The findings should therefore be interpreted as preliminary descriptive data intended to

inform future, larger-scale studies aimed at quantifying anatomical variability and validating the porcine model for broader translational and training applications. Secondly, all radiological measurements were performed by a single experienced radiologist, and intra- or inter-observer variability was not formally assessed. Although predefined anatomical landmarks and standardised measurement techniques were used to enhance consistency, the absence of repeatability analysis limits assessment of measurement reproducibility. Future studies incorporating multiple observers and formal variability analysis would strengthen validation of the morphometric findings.

5. Conclusions

While there are numerous similarities between the urinary systems of humans and pigs, comparative anatomical descriptions highlight small but clinically important differences that urologists and researchers must recognise. By integrating computed tomography (CT) with direct endoscopic evaluation, this study provides a comprehensive anatomical correlation that enhances procedural understanding and translational accuracy.

These findings are directly relevant to endourology training and retrograde intrarenal surgery (RIRS), where precise knowledge of ureteral and intrarenal anatomy influences access, navigation, and experimental reproducibility. The authors were able to use the insights gained from this work to conduct meaningful studies in endourology that advance the surgical management of patients with nephrolithiasis [8,9]. A structured, multimodal understanding of porcine urinary anatomy is therefore essential to optimise training fidelity, strengthen translational research, and ensure safe and effective innovation in stone surgery.

Author Contributions: Conceptualization, J.J.; methodology, J.J.; formal analysis, J.J.; investigation, J.J.; resources, J.L.; writing—original draft preparation, J.J.; writing—review and editing, L.K., G.F., J.L.; funding acquisition, J.L. All authors have read and agreed to the published version of the manuscript.

Funding: This study was supported by the National Center for Research and Development (Project No. M-ERA.NET2/2019/1/2020) and the Department of Science and Innovation, South Africa within the "IsoWire" project under the M-ERA.NET Program (Call2019) cofinanced by the European Union.

Institutional Review Board Statement: The animal study protocol was approved by the University of Cape Town (UCT) Department of Surgery Research Committee and Animal Ethics Committee (AEC 020_011) on 30 January 2023.

Informed Consent Statement: Not applicable.

Data Availability Statement: Raw data is available from the corresponding author on reasonable request.

Conflicts of Interest: The authors declare no conflicts of interest.

Abbreviations

The following abbreviations are used in this manuscript:

CT	Computed tomography
AEC	Animal ethics committee
kg	kilograms
mg/kg	milligrams per kilogram
IM	intramuscular
mL	millilitre
mL/kg	millilitre per kilogram
mL/kg/h	millilitre per kilogram per hour
ROI	region of interest

Fr	French
SPSS	Statistical Package for the Social Sciences
cm	centimetre
cm^3	cubic centimetres
cc	cubic centimetre
SD	standard deviation
CV	coefficient of variation

References

1. Lee, K.H.; Lee, D.W.; Kang, B.C. The 'R' principles in laboratory animal experiments. *Lab. Anim. Res.* **2020**, *36*, 45. [CrossRef] [PubMed]
2. Smith, K.A. Edward Jenner and the Small Pox Vaccine. *Front. Immunol.* **2011**, *2*, 21. [CrossRef] [PubMed]
3. Cooper, D.K. Christiaan Barnard—The surgeon who dared: The story of the first human-to-human heart transplant. *Glob. Cardiol. Sci. Pract.* **2018**, *2018*, 11. [CrossRef] [PubMed]
4. Bushi, D.; Assaf, Y.; Grad, Y.; Nishri, B.; Yodfat, O.; Tanne, D. Similarity of the Swine Vasculature to the Human Carotid Bifurcation: Analysis of Arterial Diameters. *J. Vasc. Interv. Radiol.* **2008**, *19*, 245–251. [CrossRef]
5. Smith, A.C.; Swindle, M.M. Preparation of Swine for the Laboratory. *ILAR J.* **2006**, *47*, 358–363. [CrossRef]
6. Gómez, F.A.; Ballesteros, L.E.; Estupiñán, H.Y. Anatomical study of the renal excretory system in pigs. A review of its characteristics as compared to its human counterpart. *Folia Morphol.* **2017**, *76*, 262–268. [CrossRef]
7. Sampaio, F.J.B.; Pereira-Sampaio, M.A.; Favorito, L.A. The Pig Kidney as an Endourologic Model: Anatomic Contribution. *J. Endourol.* **1998**, *12*, 45–50. [CrossRef]
8. John, J.; Wellman, M.; Kellermann, T.; Kopeć, K.; Ciach, T.; Fieggen, G.; Kaestner, L.; Lazarus, J. Pharmacological Modulation of Intrarenal Pressure in a Porcine Model Using a Novel Isoprenaline-Eluting Guidewire. *J. Endourol.* **2024**, *38*, 1185–1191. [CrossRef]
9. John, J.; Wellman, M.; Dixon, C.; Kellermann, T.; Wisniewski, P.; Kopeć, K.; Trzciński, J.; Kopeć, D.; Ciach, T.; Fieggen, G.; et al. Introducing an isoprenaline eluting guidewire—Report on its design and the results of the dose-determining pilot study. *J. Endourol.* **2024**, *38*, 590–597. [CrossRef]
10. Lildal, S.K.; Hansen, E.S.S.; Laustsen, C.; Nørregaard, R.; Bertelsen, L.B.; Madsen, K.; Rasmussen, C.W.; Osther, P.J.S.; Jung, H. Gadolinium-enhanced MRI visualizing backflow at increasing intra-renal pressure in a porcine model. *PLoS ONE* **2023**, *18*, e0281676. [CrossRef] [PubMed]
11. Jakobsen, J.S.; Jung, H.U.; Gramsbergen, J.B.; Osther, P.J.; Walter, S. Endoluminal isoproterenol reduces renal pelvic pressure during semirigid ureterorenoscopy: A porcine model. *BJU Int.* **2010**, *105*, 121–124. [CrossRef]
12. Raison, N.; Poulsen, J.; Abe, T.; Aydin, A.; Ahmed, K.; Dasgupta, P. An evaluation of live porcine simulation training for robotic surgery. *J. Robot. Surg.* **2021**, *15*, 429–434. [CrossRef]
13. Glodny, B.; Unterholzner, V.; Taferner, B.; Hofmann, K.J.; Rehder, P.; Strasak, A.; Petersen, J. Normal kidney size and its influencing factors—A 64-slice MDCT study of 1.040 asymptomatic patients. *BMC Urol.* **2009**, *9*, 19. [CrossRef]
14. Karami, M.; Rahimi, F.; Tajadini, M. The evaluation and comparison of kidney length obtained from axial cuts in spiral CT scan with its true length. *Adv. Biomed. Res.* **2015**, *4*, 19. [CrossRef]
15. Emamian, S.A.; Nielsen, M.B.; Pedersen, J.F.; Ytte, L. Kidney dimensions at sonography: Correlation with age, sex, and habitus in 665 adult volunteers. *Am. J. Roentgenol.* **1993**, *160*, 83–86. [CrossRef]
16. Arenas, F.; Rincón, J.; Álvarez, J.C.; Gómez, F.A.; Cortés, L.S. Contribution to the Anatomical Study of Urinary System in Pigs. *Spei Domus* **2015**, *11*, 17–24. [CrossRef]
17. Gómez, F.A.; Ballesteros, L.E.; Estupiñan, H.Y. Morphological Characterization of the Renal Arteries in the Pig: Comparative Analysis with the Human. *Int. J. Morphol.* **2017**, *35*, 319–324. [CrossRef]
18. Kalucki, S.A.; Lardi, C.; Garessus, J.; Kfoury, A.; Grabherr, S.; Burnier, M.; Pruijm, M. Reference values and sex differences in absolute and relative kidney size. A Swiss autopsy study. *BMC Nephrol.* **2020**, *21*, 289. [CrossRef] [PubMed]
19. Smit, J.H.A.; Leonardi, E.P.; de Figueiredo Chaves, R.H.; Furlaneto, I.P.; da Silva, C.M.S.; de Campos Vieira Abib, S.; de Oliveira Góes Junior, A.M. Image-guided study of swine anatomy as a tool for urologic surgery research and training. *Acta Cir. Bras.* **2020**, *35*, e351208. [CrossRef] [PubMed]
20. Talhar, S.S. Computed Tomographic Estimation of Relationship between Renal Volume and Body Weight of an Individual. *J. Clin. Diagn. Res.* **2017**, *11*, AC04–AC08. [CrossRef]
21. Pereira-Sampaio, M.A.; Favorito, L.A.; Sampaio, F.J.B. Pig kidney: Anatomical relationships between the intrarenal arteries and the kidney collecting system. Applied study for urological research and surgical training. *J. Urol.* **2004**, *172*, 2077–2081. [CrossRef]
22. Satyapal, K.S.; Haffejee, A.A.; Singh, B.; Ramsaroop, L.; Robbs, J.V.; Kalideen, J.M. Additional renal arteries incidence and morphometry. *Surg. Radiol. Anat.* **2001**, *23*, 33–38. [CrossRef]

23. Evan, A.P.; Connors, B.A.; Lingeman, J.E.; Blomgren, P.; Willis, L.R. Branching patterns of the renal artery of the pig. *Anat. Rec.* **1996**, *246*, 217–223. [CrossRef]
24. Sampaio, F.J.B.; Aragao, A.H.M. Anatomical Relationship Between the Intrarenal Arteries and the Kidney Collecting System. *J. Urol.* **1990**, *143*, 679–681. [CrossRef]
25. Tunc, L.; Resorlu, B.; Unsal, A.; Oguz, U.; Diri, A.; Gozen, A.S.; Bedir, S.; Ozgok, Y. In vivo Porcine Model for Practicing Retrograde Intrarenal Surgery. *Urol. Int.* **2014**, *92*, 64–67. [CrossRef] [PubMed]
26. Shehata, R. A comparative study of the urinary bladder and the intramural portion of the ureter. *Cells Tissues Organs* **1977**, *98*, 380–395. [CrossRef]
27. Ozturk, N.K.; Kavakli, A.S. The use of bladder volume measurement assessed by ultrasound in predicting postoperative urinary retention. *North. Clin. Istanb.* **2016**, *3*, 209–216. [CrossRef] [PubMed]
28. Dalmose, A.L.; Hvistendahl, J.J.; Olsen, L.H.; Eskild-Jensen, A.; Djurhuus, J.C.; Swindle, M.M. Surgically Induced Urologic Models in Swine. *J. Investig. Surg.* **2000**, *13*, 133–145. [CrossRef] [PubMed]
29. Swindle, M.M.; Makin, A.; Herron, A.J.; Clubb, F.J., Jr.; Frazier, K.S. Swine as Models in Biomedical Research and Toxicology Testing. *Vet. Pathol.* **2012**, *49*, 344–356. [CrossRef]

Disclaimer/Publisher's Note: The statements, opinions and data contained in all publications are solely those of the individual author(s) and contributor(s) and not of MDPI and/or the editor(s). MDPI and/or the editor(s) disclaim responsibility for any injury to people or property resulting from any ideas, methods, instructions or products referred to in the content.